

4-11 Observation of the tropospheric aerosol by using a Mie Lidar

- Observation at the arid region in China -

YASUI Motoaki, Zhou Jixia, MIZUTANI Kohei, ITABE Toshikazu, AOKI Tetsuo, and Liu Lichou

We made intensive observations of the tropospheric aerosols at Shapotou, Ningxia province, China in the period from March to May 2001. Preliminary analysis of the data shows following features. (1) A dense atmospheric dust layer was always existed in the lowest troposphere which top was 2 - 3 km above the ground surface. It is considered that the layer corresponded to the local mixing layer. (2) Distinct dust layers sometimes appeared at height around 4 or 5km. It is considered that these layers were on the way of long-range transport. (3) In May, there was a case that tops of the local dust layer reached up to height around 5km. In such a condition, injection of the dust into free atmosphere might have occurred easily. (4) Generally, aerosol optical depth was small in the early morning, and large in the period of afternoon to the evening. However, maximum optical depth was observed in the midnight in several cases.

Keywords

Lidar, Aerosol, Dust, Kosa, Desert

1 Introduction

Dust particles into the atmosphere are actively injected in the arid regions of inland China, with a steady presence of high-concentration dust layers within the lowest layer (2 to 3 km) of the mixing layer. Disturbances transport dust particles into the free atmosphere, and once injected into the free atmosphere, the dust is transported over long distances and widely dispersed. These dust particles from the arid regions of inland China are referred to as the “Kosa” in Japan, and are prevalent in the spring [Murayama et al., 2001]. The Kosa is sometimes carried over extremely long distances, and may even cross the Northern Pacific Ocean [Shaw, 1980; Merrill et al., 1989]. It is believed to strongly affect the climate over a wide region extending from the Asia-Pacific region to North America, particularly in terms of the radiative forcing of the

atmosphere. Furthermore, since most of the Kosa particles precipitate and settle in the ocean, they are considered to have a substantial effect on the marine biosphere, as a source of minerals entering into the seawater. Accordingly, the importance of dust particles in the atmosphere has been discussed from various perspectives, but its effects have yet to be quantitatively estimated, and to date there is little basic data for such studies. The results of a survey on radiative forcing by atmospheric particles have been documented in an IPCC report [IPCC (Intergovernmental Panel on Climate Change) Third Assessment Report 2001], but quantitative evaluations of the effects of dust particles (mineral dust) or of the indirect effects of clouds have yet to be performed, and many uncertainties remain. Some of the factors inhibiting the estimation of the effects of dust particles include (i) a lack of basic information on seasonal varia-

tions in ground-surface conditions, (ii) a lack of observations and an insufficient understanding of the process (and effects) of the injection of mineral particles into the atmosphere in the applicable regions, (iii) a lack of understanding of the physical properties of the dust particles, which are transformed as they are transported through the free atmosphere, and (iv) a lack of data on the three-dimensional distribution of dust particles.

In 1994, the Lidar Group of the Communications Research Laboratory (CRL) installed a lidar unit in Shapotou at the southernmost edge of the Tenger Desert, in central China. Observations using this lidar have been conducted to monitor the vertical distribution of dust particles in the local mixing layer, the amount of injection into the free troposphere, and the amount of dust particles transported by the free atmosphere above [Yasui et al., 1998(a), 1998(b)]. In 2000, the “Japan and China Joint Project on Aeolian Dust Experiment on Climate Impact (ADEC),” a research project supported by the Special Coordination Funds of the Ministry of Education, Culture, Sports, Science and Technology, was launched. The Shapotou lidar is being used in this project, and observations have been enhanced accordingly [Yasui et al., 2000]. The goals of this project are to construct a “super station” equipped with various instruments (such as a lidar, a radiometer, and a sampler) for observation over a wide area from the Taklamakan Desert in Western China to Japan, to obtain a vertical profile of dust particles at multiple sites through network observation, and to gain information on the three-dimensional distribution of dust particles based on an analysis combining the vertical distribution data with horizontal data collected by satellite observation.

Here we present the results of analysis of data from experimental observations performed in the spring of 2001, in advance of the full-scale observations scheduled to begin in the spring of 2002 [Yasui et al., 2002].

2 Observation

2.1 Observation Site (Shapotou Observation Station)

Fig.1 shows the location of Shapotou. The Shapotou Station ($37^{\circ}27'N$, $104^{\circ}57'E$; 1,250 m above sea level) of the Cold and Arid Regions Environmental and Engineering Research Institute (formerly the Lanzhou Institute of Desert Research) of the Chinese Academy of Sciences lies approximately 300 km northeast of Lanzhou in the Ningxia province. The Tenger Desert lies to the north, and to the south is the Yellow River (Fig.2). The CRL Lidar Group installed a lidar for aerosol observation within the grounds of the Shapotou Station in 1994, and has been performing observations ever since.

In this region, temperatures during the winter period (from December to mid-March) are extremely low, and the entire station is closed during this period. Therefore, observations are limited to the period from the end of March to November.

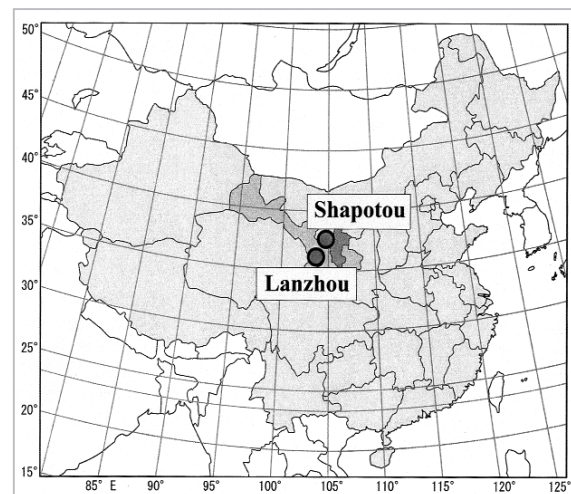


Fig.1 Location of Shapotou

Shapotou ($37^{\circ}27'N$, $104^{\circ}57'E$; 1,250 m above sea level) is located approximately 300 km northeast of Lanzhou, in the Ningxia province.

2.2 Instrumentation

Installed at Shapotou is an aerosol lidar (laser radar) that uses the second harmonic wave of the Nd:YAG laser (532 nm). The

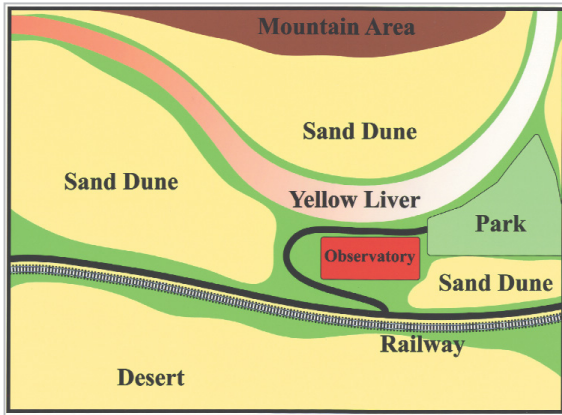


Fig.2 Geography near the observation station

The Tenger Desert lies to the north, with the Yellow River to the south.

specifications and configuration of this instrument are shown in Table 1 and Fig.3, respectively. When a laser pulse is emitted vertically into the sky with a transmitting mirror, it is scattered by aerosols and atmospheric molecules, and the components scattered in the direction of the ground (the “backscattered components”) return to the receiver system. An optical sensor in the laboratory determines the time of the laser pulse emission, and so the distance the light traveled can be calculated based on the elapsed time before the light returns. The optical quantity of the scatterer (aerosol and atmospheric molecules) can be calculated from the intensity of the received signal. The lidar’s signal-processor system consists of a signal-processing subsystem that measures the nighttime stratosphere (to approximately 30 km) using the photon-counting method, plus an A/D signal-converter subsystem for performing continuous daytime and

Table 1 Specifications of the Shapotou lidar

<i>Transmitter</i>		
Laser	Nd:YAG Laser	
Wavelength	532nm (SHG)	
Output	150mJ/Pulse	
Repetition Rate	10Hz	
Beam Divergence	0.1mrad	
Coolant	Laser Head	Water
	Power Supply	Air
<i>Receiver</i>		
Telescope	28cm (Diameter) Schmidt Cassegrain	
Field of View	1mrad	
Detector	Photomultiplier (Hamamatsu R3234)	
Signal Processing	Troposphere :	
	AD-Converting by Digital Oscilloscope (LeCroy LT224)	
	Stratosphere :	
	Photoncounting by Multi-channel Scaler (SR430)	

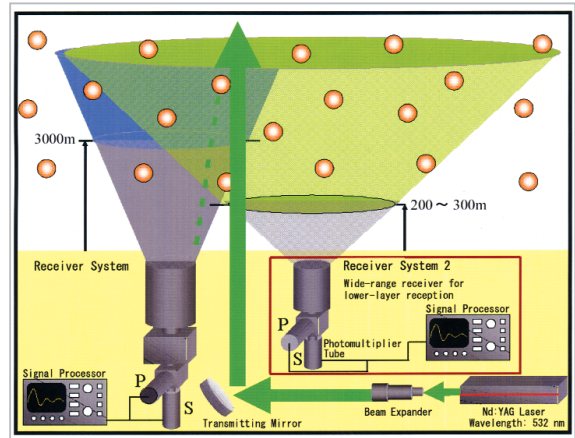


Fig.3 Schematic diagram of the lidar installed at Shapotou

Layers above 3,000 m are observed with Receiver System 1 (for middle to upper-layer observation), and layers from 200 m and above are observed with Receiver System 2 (for lower-layer observation).

nighttime troposphere measurements.

The mixing layer at the lowest level of the troposphere features high dust concentrations, which result in an extremely wide signal dynamic range. Therefore it is impossible to cover this entire range with a single receiver system designed for observations of the stratosphere. To resolve this problem, a new receiver system (Receiver System 2, shown in Fig.3) designed specifically for measurements of the lowest troposphere, was added to the lidar in August 2001. This enabled the expansion of the observation range to extend from the lowest to the upper layers by combining the observation results for the two systems (Receiver Systems 1 & 2). With full-scale observations beginning in the spring of 2002, measurements at heights of approximately 200 m will be attempted using a combination of these two receiver systems.

The results introduced in this paper are based on observations made in the spring of 2001, before the improvements to the system, and so only a single receiver system was available for observation of the area from the troposphere to the stratosphere. Therefore the lower-limit height for signal reception is 600 m.

2.3 Observation Date

The dates and times of observations from March to May 2001 are shown in Table 2.

Table 2 Date and time of observations at Shapotou from March to May 2001

Month	Date	Time
March	20	20:57 --- 24:00
	21	00:00 --- 12:57
	22	14:23 --- 24:00
	23	00:00 --- 08:23
	24	16:40 --- 24:00
	25	00:00 --- 08:40
April	26	00:00 --- 07:08
	23	13:11 --- 24:00
	24	00:00 --- 09:11
	25	19:28 --- 24:00
May	26	00:00 --- 15:28
	15	22:02 --- 24:00
	16	00:00 --- 06:02
	17	00:00 --- 02:58
18	00:00 --- 05:27	

3 Data Analysis

3.1 Data-Analysis Method for Lidar

3.1.1 A Widely Used Analysis Method for Measurements up to the Stratosphere

Normally, in analysis of lidar observation data, the backscattering coefficient $\beta(z)$, which represents the optical physical quantity of the scatterer, is determined for quantitative analysis. The relationship between the backscattering coefficient and the receiver signal $P(z)$ can be expressed by the following lidar equations.

$$P(z) = EC z^{-2} [\beta_a(z) + \beta_m(z)] T_a^2(z) T_m^2(z) \quad (1)$$

$$T_a(z) = \exp \left[- \int_0^z \sigma_a(z) dz \right] \quad (2)$$

$$T_m(z) = \exp \left[- \int_0^z \sigma_m(z) dz \right] \quad (3)$$

Here,

- z : height
- $P(z)$: signal received from height z
- E : constant for transmitted laser pulse output
- C : constant for receiver optical system
- $a(z)$: backscattering coefficient of aerosols at height z
- $m(z)$: backscattering coefficient of atmospheric molecules at height z

$T_a(z)$: transmittance of aerosols at height z

$T_m(z)$: transmittance of atmospheric molecules at height z

$a(z)$: extinction coefficient of aerosols at height z

$m(z)$: extinction coefficient of atmospheric molecules at height z

In this analysis, the backscattering coefficient was calculated using the Fernald method [Klett et al., 1981; Fernald et al., 1972; Fernald, 1984]. This method uses the following equation, obtained by transforming the lidar equation.

$$\beta_a(z) = \frac{P(z)z^2 \exp[-2(S_1 - S_2) \int_0^z \beta_m(z) dz]}{CE - 2S_1 \int_0^z P(z)z^2 \exp[-2(S_1 - S_2) \int_0^z \beta_m(z') dz'] dz} \quad (4)$$

When

$$S_1(z) = \frac{\sigma_a(z)}{\beta_a(z)} \quad (5)$$

$$S_2(z) = \frac{\sigma_m(z)}{\beta_m(z)} = \frac{8\pi}{3} \quad (6)$$

These are referred to as S -parameters. The value of the S -parameter for aerosols $S_1(z)$ depends on the particle-size distribution, shape, and complex refractive index, and varies at different points (or altitudes) in the actual atmosphere. However, when the above information is lacking, this value is often assumed to be a constant (S_1) in the calculation. Here, the value of $S_1 = 35$ (frequently used as a reference value for dust particles) was adopted [Karyampudi et al., 1999]. The S -parameter for gas molecules is constant at all heights, as evident from Equation (6).

Now let us assume that the aerosol backscattering coefficient at a certain height (calibration height) is known $\beta_a(z_c)$. Then, the relationship to the value at height z can be expressed by the following equation.

$$\beta_a(z) + \beta_m(z) = \frac{X(z) \exp \left[-2(S_1 - S_2) \int_{z_c}^z \beta_m(z) dz \right]}{\frac{X(z_c)}{\beta_a(z_c) + \beta_m(z_c)} - 2S_1 \int_{z_c}^z X(z) \exp \left[-2(S_1 - S_2) \int_{z_c}^z \beta_m(z') dz' \right] dz} \quad (7)$$

Here,

$$X(z) = P(z)z^2 \quad (8)$$

When the value for the calibration height is set, then this equation can be used to calculate the value at height z .

The initial aerosol backscattering coefficient at calibration height $a(z_c)$ was determined using the “matching method.” In this method, all signals from layers above 30 km in the mid-latitude regions are assumed to be due to Rayleigh scattering by atmospheric molecules since there are almost no aerosols at such heights. The received signal profiles are then matched with a theoretically calculated Rayleigh scattering profile for signal calibration. Rayleigh scattering components are calculated using an atmospheric-density profile calculated from height distribution data of temperature and pressure collected through observations with instruments such as a radio sonde. The present analysis uses the sounding data available at the website of the University of Wyoming (<http://weather.uwyo.edu/>). Furthermore, the transmittance terms in the lidar equation (Equation (2) & Equation (3)) were both assumed to have a value of 1 in the estimation of the aerosol backscattering coefficient at calibration height. In other words, the constants E and C in the lidar equation are eliminated by matching, and by assuming that transmittance is 1, the initial value of the ratio of scattering at calibration height Rc is determined using the equation below.

$$R(z_c) = \frac{\beta_a(z_c) + \beta_m(z_c)}{\beta_m(z_c)} \quad (9)$$

Since the backscattering coefficient for atmospheric molecules $m(z_c)$ can be theoretically determined from atmospheric density distribution, the initial value for backscattering coefficient of aerosol $a(z_c)$ is determined by the value $m(z_c)$ and Equation (4). In the actual analysis, the atmosphere is divided into multiple layers in the vertical direction (resolution of z), and the vertical profile is determined by successively calculating the value for the next lower layer beginning at the calibration height. In other words, the aerosol

backscattering coefficient $a(z_c - z)$ is first calculated for the layer directly below the calibration layer using the value at calibration height $a(z_c)$. Then the obtained value $a(z_c - z)$ is used to calculate the coefficient for the next lower layer $a(z_c - 2z)$, and so on, to determine the vertical profile of $a(z)$.

3.1.2 Analyses of Results of Continuous Daytime and Nighttime Tropospheric Observation

The matching method in the previous section can only be applied to data analysis for the stratosphere above an altitude of 30 km, where signals due to aerosols can be ignored. With the present system, observations up to the stratosphere cannot be made during the daytime due to high levels of background noise from sunlight. Even for nighttime observations, there are many cases in which the matching method cannot be applied due to low signal level from the stratosphere when optically thick layers (e.g., layers dense with clouds) are present in the troposphere. However, observations of daily variations are extremely important in tropospheric dust observations, and so observation is continued day and night, regardless of cloud conditions. Therefore, an effective method must be found for analysis of daytime data when observations cannot be performed of areas up to the stratosphere. In the process of lidar data analysis at Shapotou, valid data from observations up to the stratosphere is selected from nighttime data, standardization is performed using the matching method, and the results are then used to determine the instrumental constants (E and C in Equation (1)). These constants are then used for standardization of all data, including daytime data. Next, the initial value of the backscattering coefficient at calibration height is calculated, and then the Fernald method is applied.

3.2 Treatment of the Lowermost Layer

With the present lidar instrument configuration, observation cannot be made for the section from the ground to a height of 600 m because the transmitted light does not fall

completely within the field-of-view of the receiver system. The aerosol concentration in the lower atmosphere tends to increase exponentially in the lower layers, and so it is highly likely that dust particles are present in significantly large volumes in the section between the ground and a height of 600 m, a section that cannot be observed using the present lidar unit. The volume of this unobservable section was tentatively estimated by extrapolation (based on the shape of the profile for layers above 600 m) for regions where exponential extrapolation was considered appropriate for the lowermost layer (Fig.4). The results of extrapolation are shown in Fig.5 for reference. Where the profile featured a complex shape and exponential extrapolation seemed inappropriate, extrapolation was not performed (shaded areas in Fig.5) and analysis was limited to layers above a height of 600 m.

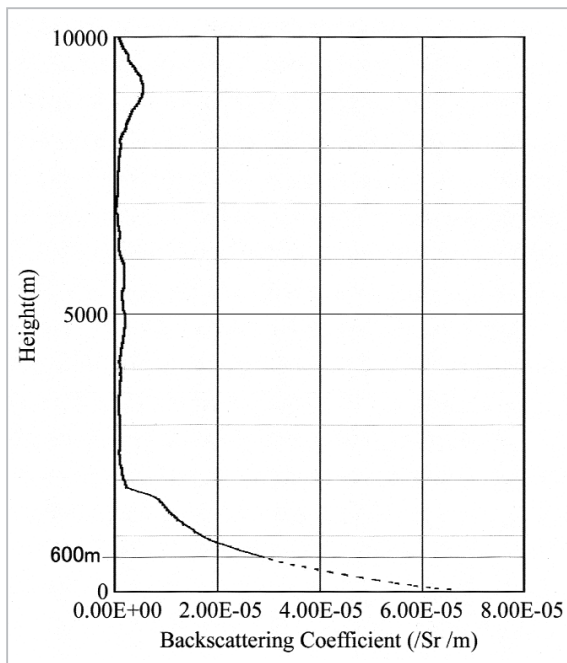


Fig.4 Example of extrapolation of the lowermost layer for the vertical profile of the backscattering coefficient

When the profile in the 600 to 1,000-m range seems to follow an exponential curve, the section between the ground and a height of 600 m was calculated by extrapolation.

4 Results and Discussions

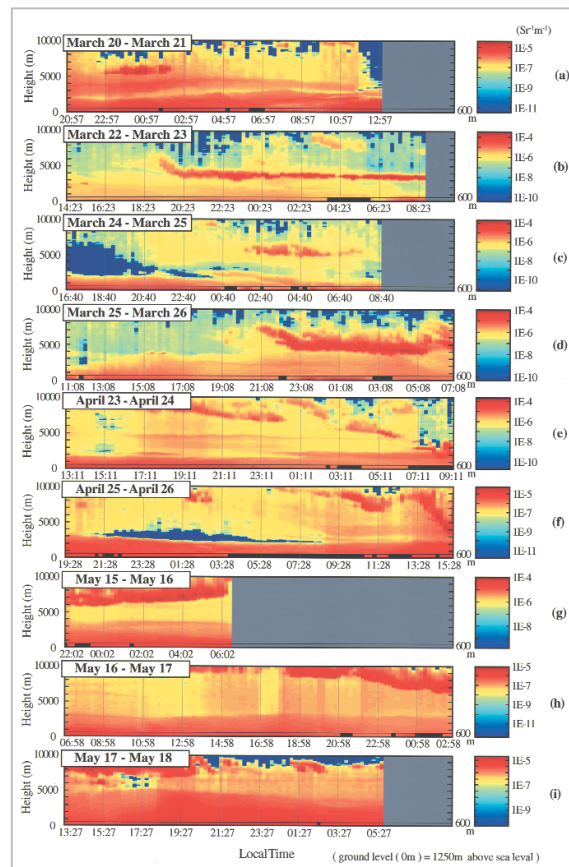


Fig.5 The time-height cross-section of the vertical profile of the backscattering coefficient in March, April, and May 2001

The horizontal and vertical axes represent local time and geometric height from the ground, respectively. Since Shapotou is 1,250 m above sea level, add 1,250 m to the plotted value for the elevation above sea level.

4.1 Vertical Profile of the Backscattering Coefficient

Fig.5 is a time-height cross-section of the aerosol backscattering coefficients between the ground and an altitude of 10 km, calculated from the results of observations in March, April, and May 2001. The dotted lines at the lowermost layer in each plot represent a height of 600 m, and as stated previously, values for layers below this level are not based on actual observation but rather represent extrapolated values assuming an exponential distribution. Where exponential extrapolation seemed to be inappropriate, the values were not calculated and the applicable section was shaded. The layers of strong scattering, which appear frequently at upper layers above an altitude of 5

km (near 4 km in the case of Fig.5(b)), are caused by clouds. Clouds were distinguished from dust layers based on temporal variations in the intra-layer structures.

Fig.6 shows the values of extinction coefficients integrated in the vertical direction based on results of observation from March 25 to 26, and the calculation results are presented for the height ranges of 0.6 to 5 km and 0.6 to 10 km. The values indicate the optical depth of the particle layer in the two ranges. In this example, no clouds are present in the first 600 (50 × 12) minutes after start of observation, and only aerosol particle layers are observed. After 600 minutes, clouds start to appear, and there is a sharp increase in optical depth. Furthermore, the cloud layer displays rapid short-term variations in optical depth, which are believed to be caused by internal structures characteristic of clouds. Such distinctive short-term variations are frequently observed in clouds. In the present analysis, all clouds were successfully identified in this manner.

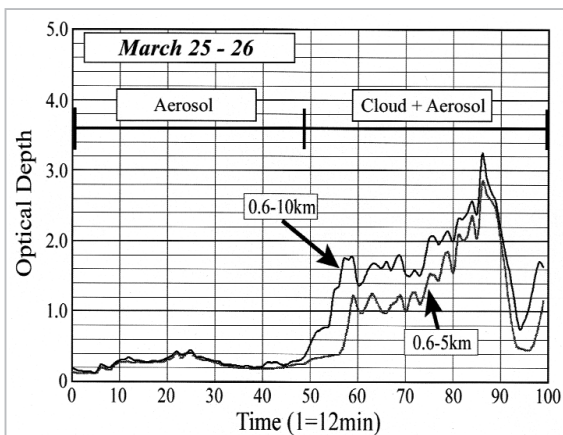


Fig.6 Distinguishing cloud from aerosol layer. Sample data for March 25 and 26

Aerosol optical depths at 0.6 to 5 km and at 0 to 10 km are plotted. The aerosol optical depth is relatively stable with time, while the cloud layer changes drastically within a short time. These characteristics were used to distinguish between cloud and aerosol layers.

The common characteristic of all plots in Fig.5 is the existence of a dust-particle layer in the lowermost troposphere with a ceiling at 2 to 3 km. This layer most likely corresponds to the local mixing layer, and when transport to

upper layers due to disturbances are small, most of the atmospheric dust particles are believed to remain within this layer. Layered structure within the mixing layer displays large variations, and in Fig.5(c), it shifts downwards from around 1:00 AM to dawn, while in Fig.5(a), it shifts upward before dawn at 3:00 to 4:00 AM, suggesting active motion not only in the daytime but also during the night.

Besides those in the mixing layer, dust layers were also observed at altitudes between 4 and 5 km. In observations on March 20 to 21, a layer centered at approximately 4 km was found to persist for a long time (Fig.5(a)). This dust layer existed separately from that in the mixing layer, and maintained a relatively stable condition. This implies that this layer consisted of dust particles injected into the free atmosphere at some other location and transported into this region by winds in the free atmosphere. A similar layer is also noted from observations on April 23 to 24 (Fig.5(e)).

Among the observations in May, a single, thick layer reaching up to an altitude of nearly 5 km is seen in observations from the afternoon of May 17 to the early morning of May 18 (Fig.5(i)), indicating that favorable conditions existed for dust-particle injection into the free troposphere.

4.2 Optical Depth of the Dust Particle Layer

4.2.1 Optical Depth from 0.6 km to 5 km

Fig.7 shows the results of optical depth calculation for heights between 0.6 km and 5 km. Regions with extremely large values are caused by clouds (Fig.7(b), (d), (e), and (f)). Fig.8(a) shows the frequency distribution of the ratio (in percent) of the aerosol optical depth between 0.6 km and 5 km ($AOD_{0.6-5km}$) to that between 0.6 km and 10 km ($AOD_{0.6-10km}$). These are results for cloudless regions selected from all observations from March to May. It was found that approximately 70% or more of the aerosols optical depth was due to aerosols between 0.6 km and 5 km.

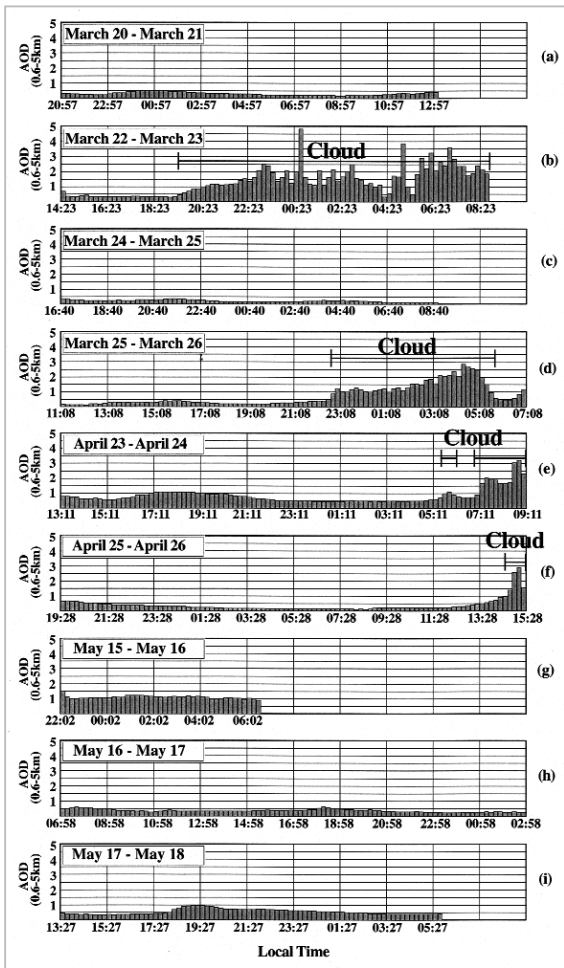


Fig.7 Temporal variations of aerosol optical depth at 0.6 to 5 km ($AOD_{0.6-5km}$)

Extremely large values are due to clouds. Generally, $AOD_{0.6-5km}$ is large from the afternoon to dusk, and small in early morning. However, in several instances, the maximum was observed near midnight ((a) & (c)).

According to Fig.7, $AOD_{0.6-5km}$ is generally large from the afternoon to dusk, and low in the early morning. Such daily variations are considered to result from changes in solar elevation, and may reflect the characteristics of a typical daily variation on a relatively calm, clear day. In this scenario, dust particles are carried upward by thermals created by solar heating of the ground in the daytime; then, relatively large dust particles carried upward in this manner settle at night due to gravity, leading to the formation of a stable stratification due to radiational cooling in the lower atmosphere.

However, in some cases, maximum optical

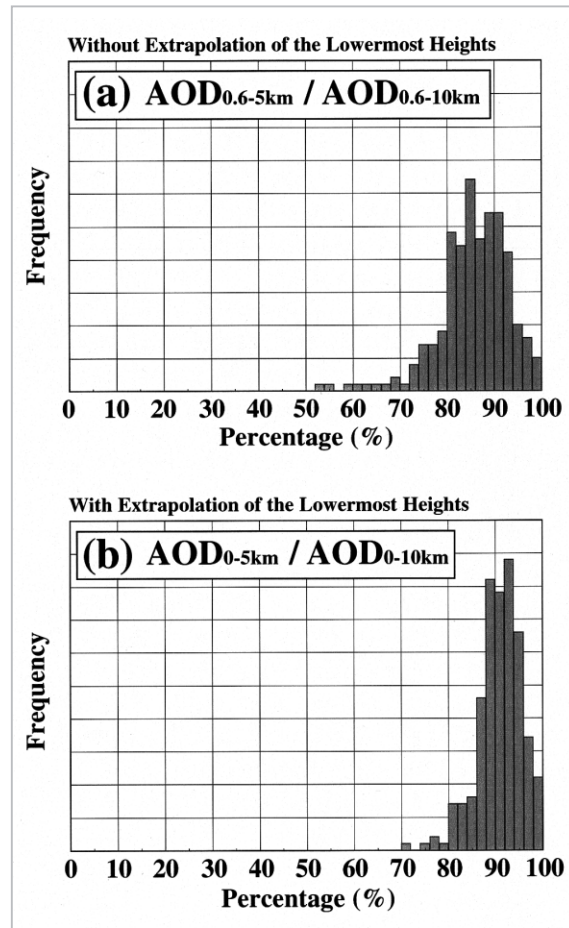


Fig.8 (a) Frequency distribution of the ratio (in percent) of the aerosol optical depth between 0.6 km and 5 km to that between 0.6 km and 10 km (b). Frequency distribution of the ratio (in percent) of the aerosol optical depth between 0 km and 5 km height to that between 0 km and 10 km

Data for observations involving clouds were excluded from the data observed between March and May to select for aerosol-only data.

depths were observed near midnight (Fig.7(a), (c)), which suggests the possibility that some form of upward movement of dust particles occurs at night. To gain insight into such phenomena, it is essential to conduct continuous 24-hour monitoring.

4.2.2 Optical Depth Between Ground and an altitude of 5 km (Results of Extrapolation)

Fig.9 shows the results of optical depth calculations by extrapolation for the section between the ground and an altitude of 5 km, for which lidar observations cannot be made, and Fig.8(b) shows the frequency distribution

of the ratio (in percent) of the aerosol optical depth between 0 km and 5 km (AOD_{0-5km}) to that between 0 km and 10 km (AOD_{0-10km}). The general trend is similar to the case of $AOD_{0.6-5km}$, although there were some cases where significantly high concentrations of dust particles were believed to be present in the lowermost extrapolated layer (Fig.9(c), (e), (g)). Fig.8(b) also indicates that, when the lowermost layer near the ground is included, approximately 80% or more of the aerosol optical depth of troposphere is considered to be due to aerosols existing below 5 km.

5 Conclusions

From March to May 2001, lidar observations were made to obtain vertical profiles of the tropospheric dust layer in Shapotou, China. The following results were obtained through a preliminary analysis of data.

- (1) A high-concentration dust layer is constantly present with a ceiling at a height of 2 to 3 km. This layer is believed to correspond to the local mixing layer. Active changes are seen in the structure of the dust layer in the mixing layer not only in the daytime but also at night.
- (2) Dust-particle layers were sometimes observed in the free atmosphere at heights near 4 to 5 km. Most of these layers were completely independent of the dust layers within the local mixing layer, and are considered to have been transported above Shapotou after being injected into the free atmosphere at another location.
- (3) On May 17 and 18, a continuous, thick layer stretching from the mixing layer up to an altitude of nearly 5 km was observed, and it is believed that conditions were favorable for injection of dust particles from the mixing layer into the free atmosphere.
- (4) The aerosol optical depth, $AOD_{0.6-5km}$, was generally large from the afternoon to dusk, and small in the early morning. However, in several instances, the maximum was observed near midnight. Such midnight

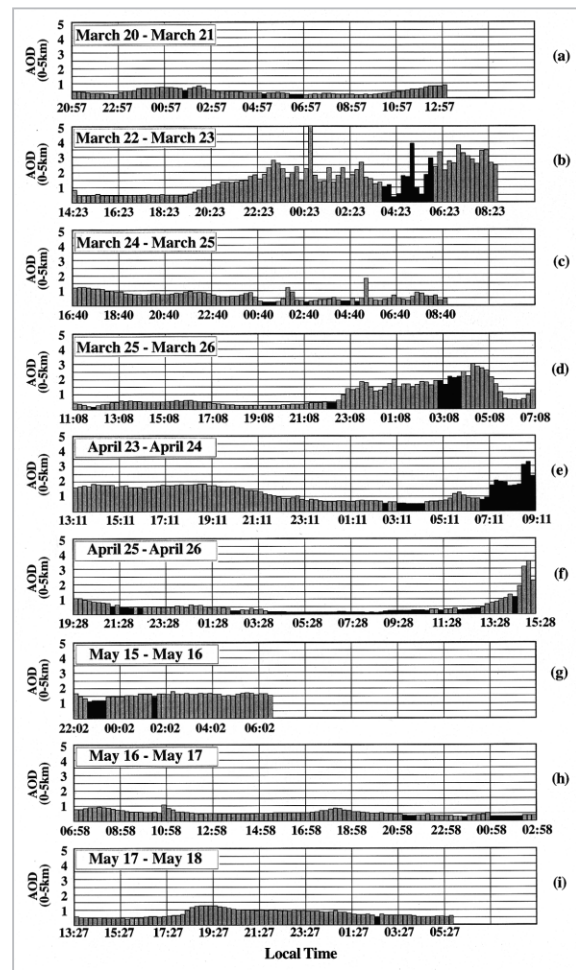


Fig.9 Temporal variations in the aerosol optical depth between 0 and 5 km (AOD_{0-5km})

The values between 0 and 0.6 km are results of extrapolation. The shaded areas in the figure represent cases in which extrapolation seemed inappropriate; therefore, values for this range are not included in the calculation (i.e., for the filled areas, the values are the same as those in Fig.7.) As with Fig.7, extremely large values are due to clouds.

maximum cannot be explained by simple daily variations of dust-particle layers in the mixing layer due to solar elevation.

Acknowledgments

This study was supported by the Special Coordination Funds of the Ministry of Education, Culture, Sports, Science and Technology. Research activities in China were conducted jointly with the Chinese Academy of Sciences. We are grateful to all those involved.

References

- 1 G. E. Shaw, "Transport of Asian desert aerosol to the Hawaiian Islands", *J. Appl. Meteor.*, 19, 1254-1259, 1980.
- 2 IPCC (Intergovernmental Panel on Climate Change) Third Assessment Report 2001.
- 3 J. T. Merrill, M. Uematsu, and R. Bleck, "Meteorological analysis of long range transport of mineral aerosols over the North Pacific", *J. Geophys. Res.*, 94, 8584-8598.
- 4 J. D. Klett, "Stable analytical inversion solution for processing lidar returns", *Appl. Opt.*, 20, 211-220, 1981.
- 5 F. G. Fernald, B. M. Herman, and J. A. Reagan, "Determination of Aerosol Height Distributions by Lidar", *J. Appl. Meteor.*, 11, 482-489, 1972.
- 6 F. G. Fernald, "Analysis of atmospheric lidar observations: some comments", *Appl. Opt.*, 23, 652-653, 1984.
- 7 M. Yasui, K. Mizutani, T. Itabe, M. Takabe, J. Zhou, Y. Ling, and L. Liu, "Lidar Observation of Tropospheric Aerosols at Lanzhou in China", *J. Arid Land Studies*, 7-2, 169-173, 1998(a).
- 8 M. Yasui, K. Mizutani, T. Itabe, M. Takabe, J. Zhou, Y. Ling, and L. Liu, "Lidar Observation of Atmospheric Aerosol Particles at Lanzhou in China", *J. Arid Land Studies*, 8-2, 177-180, 1998(b).
- 9 M. Yasui, K. Tsuchiya, K. Kai, T. Uehara, T. Ootomo, T. Nagai, K. Mizutani, J. Miyamoto, A. Itou, M. Nakazato, and A. Ichiki, "Observational and Analytical Studies on the Mechanism of the Long-Range Transport of Aeolian Dust", *J. Arid Land Studies*, 10-3, 238-245, 2000.
- 10 M. Yasui, J. Zhou, L. Liu, T. Itabe, K. Mizutani, and T. Aoki, "Lidar Measurements of the Airborne Dusts in Shapotou - Preliminary Results in the springtime 2001", *J. Arid Land Studies*, 2002, printing.
- 11 T. Murayama, N. Sugimoto, I. Uno, K. Kinoshita, K. Aoki, N. Hagiwara, Z. Liu, I. Matsui, T. Sakai, T. Shibata, K. Arao, B. Sohn, J. Won, S. Yoon, T. Li, J. Zhou, H. Hu, M. Abo, K. Iokibe, R. Koga, and Y. Iwasaka, "Ground-based network observation of Asian dust events of April 1998 in east Asia", *J. Geophys. Res.*, 106, 18345-18359, 2001.
- 12 V. M. Karyampudi, S. P. Palm, J. A. Reagen, H. Fang, W. B. Grant, R. M. Hoff, C. Moulin, H. F. Pierce, O. Torres, E. V. Browell, and S. H. Melfi, "Validation of the Saharan Dust Plume Conceptual Model Using Lidar, Meteosat, and ECMWF Data", *Bul. Amer. Meteor. Soc.*, 80, 1045-1075, 1999.



YASUI Motoaki, Dr. Sci.

*Senior Researcher, Lidar Group,
Applied Research and Standards Division*

Atmospheric Science



MIZUTANI Kohei, Ph. D.

*Leader, Lidar Group, Applied Research
and Standards Division*

Laser Remote Sensing



AOKI Tetsuo, Ph. D.

*Senior Researcher, Lidar Group,
Applied Research and Standards Division*

*Optical Remote Sensing, Infrared
Astronomy*

Zhou Jixia

*Associate Professor, Cold and Arid
Regions Environmental and Engineering
Research Institute, Chinese Academy
of Sciences*

Atmospheric Science, Arid Land Science

ITABE Toshikazu, Ph. D.

*Executive Director, Basic and Advanced
Research Division*

Laser Remote Sensing

Liu Lichou

*Research Associate, Cold and Arid
Regions Environmental and Engineering
Research Institute, Chinese Academy
of Sciences*

Atmospheric Science, Arid Land Science